

# Phosphate-containing metabolites switch on phosphorescence of ferric ion engineered carbon dots in aqueous solution†

Cite this: *RSC Adv.*, 2014, 4, 22318

Xiao Yan,<sup>‡a</sup> Jin-Long Chen,<sup>‡\*ab</sup> Meng-Xiang Su,<sup>ab</sup> Fang Yan,<sup>ab</sup> Bo Li<sup>ab</sup> and Bin Di<sup>\*ab</sup>

While most research has focused on the development of carbon dot (CD) based fluorescence sensors, much less attention has been paid to the phosphorescence phenomenon and its potential applications to date. Herein, room temperature phosphorescence (RTP) of water soluble CDs free of deoxidants and other inducers was observed for the first time in pure aqueous solution. RTP of CDs could be significantly quenched when chelating with iron ions as well as aggregation of CDs, presumably resulting from the formation of non-luminescent chelate. Due to a high affinity of iron ions to phosphate ions through well-known Fe–O–P bonds, the quenched RTP of functionalized CDs by Fe<sup>3+</sup> could be basically recovered in the presence of phosphate-containing molecules. For a proof-of-concept demonstration, adenosine-5'-triphosphate (ATP), as a common phosphate-containing metabolite was quantitatively detected by a phosphorescence “off-to-on” approach. The enhancement of RTP at 440 nm was linearly proportional to the concentrations of ATP ranging from 20 to 200 μM with a detection limit as low as 14 μM. Moreover, the iron ion engineered CDs based RTP probe was used to estimate ATP levels in human blood plasma.

Received 24th March 2014  
Accepted 11th April 2014

DOI: 10.1039/c4ra02592j

www.rsc.org/advances

## Introduction

Carbon dots (CDs) have attracted much attention in recent years, owing to advantages such as excellent optical properties, low toxicity, good biocompatibility, hydrophilicity and simple synthesis.<sup>1–4</sup> While most researches focus on the development of CD based on fluorescence, phosphorescence properties have been paid much less attention. Room temperature phosphorescence (RTP) has been increasingly applied in sensing, bio-imaging and anti-counterfeiting.<sup>5–7</sup> On account of the emission delay, phosphorescence detection possesses a significant advantage in that any fluorescence emission and scattering light could be stopped simply. In addition, only very few compounds are able to emit analytically useful phosphorescence at room temperature.<sup>8</sup> As is well known, RTP generally originates from inorganics or metal complexes which might represent a serious limitation due to known toxicity, potential environment hazards and costliness.<sup>9–11</sup> RTP emitted by CDs, until now, has been observed only in assistant with the

perturbation of a heavy atom, or on a solid support.<sup>12,5</sup> However, RTP emission from CDs dispersed in water has not been reported before. Interestingly, we have found that phosphorescence emissions can be observed in CDs dispersed in water at room temperature.

Phosphate-containing metabolites, which include nucleoside pyrophosphates, pyrophosphates, phosphates and phosphoproteins, play critical roles in biological processes.<sup>13</sup> The level of phosphate-containing metabolites can be used as an indication of the orderly condition of biological systems. For example, adenosine-5'-triphosphate (ATP), an extracellular signaling agent and the major energy carrier in cells, which has not only been used as an indicator of cell viability, but also associated with particular diseases such as angiocardopathy due to excessive production of ATP by creatine kinase.<sup>14–16</sup> In general, the physiological concentration of blood phosphate is at a millimolar level, which mainly consists of ATP.<sup>17</sup> Although the traditional methods for determination of ATP levels *in vitro* such as the luciferase assay, are sensitive, the enzyme and substrates are costly and of uncertain stability.<sup>18</sup> Considerable efforts have been devoted towards designing a fluorescence probe to detect phosphorylated species, but the fluorescence might face interference due to the scattering of light or fluorescence from matrixes.<sup>19–21</sup>

Herein, we demonstrate for the first time a phosphorescence “off-to-on” approach for sensing ATP by utilization of functionalized CDs. The phosphorescence of CDs is significantly quenched when chelating with iron ions, then they are “turned-

<sup>a</sup>Department of Pharmaceutical Analysis, China Pharmaceutical University, Nanjing 210009, China. E-mail: dibin@cpu.edu.cn; ddw888@vip.sina.com; Fax: +86 2583271269; Tel: +86 2593271269

<sup>b</sup>Key Laboratory of Drug Quality Control and Pharmacovigilance, China Pharmaceutical University, Ministry of Education, Nanjing 210009, China

† Electronic supplementary information (ESI) available. See DOI: 10.1039/c4ra02592j

‡ Jin-Long Chen and Xiao Yan contributed equally to this work.

on" in the presence of phosphorylated species. Since ATP is the main phosphate-containing metabolite in plasma, the proposed sensing assay can be successfully used to rapidly estimate the levels of phosphate-containing metabolites in plasma.

## Experimental section

### Materials and apparatus

Citric acid, ethylenediamine, ferric trichloride hexahydrate ( $\text{FeCl}_3 \cdot 6\text{H}_2\text{O}$ ), tris(hydroxymethyl)aminomethane were of analytical grade and used without further purification. Adenosine 5'-triphosphate (ATP) disodium trihydrate was purchased from Sigma-Aldrich and kept in the freezer under  $-20\text{ }^\circ\text{C}$ . Human blood plasma was kindly provided by China Pharmaceutical University Hospital Department. All aqueous solutions were prepared with deionized water purified through PL5242 Purelab Classic UV (PALL Co. Ltd., USA) to a resistivity of  $18.2\text{ M}\Omega\text{ cm}$ .

### Instrumentation

Phosphorescence measurements were performed on a Hitachi F-4600 spectrofluorometer (Hitachi Co. Ltd., Japan) in the phosphorescence mode. Transmission electron microscopy (TEM) images were obtained from a TECNAI G2 F20 (FEI Co., USA). UV-Vis absorption spectra were recorded with a Shimadzu UV-2401 PC instrument (Shimadzu Co. Ltd., Japan). The FT-IR spectra ( $4000\text{--}400\text{ cm}^{-1}$ ) in KBr were collected on a Jasco FT-IR-4100 spectrometer (Jasco Co. Ltd., Japan). Time-resolved fluorescence and phosphorescence decay by delay were performed on a FluoroMax-4 spectrofluorometer (Horiba Jobin Yvon Co. Ltd., France).

### Preparation of phosphorescent CDs

Modifying from the previous work,<sup>22</sup> 0.42 g of citric acid and 535  $\mu\text{L}$  of ethylenediamine were dissolved in 10 mL of deionized water. Then the solution was transferred to a Teflon-lined stainless autoclave and heated at  $200\text{ }^\circ\text{C}$  for 5 hours. The reactor was cooled to room temperature, the resultant CDs solution was purified by silica gel column with water as the developing solvent. The purified CD solution was freeze-dried under vacuum. Finally, the brown-black hygroscopic CDs were obtained and stored in a dark desiccator at room temperature.

### Phosphorescence measurement

The "on-off-on" alternation of the phosphorescence of CDs was performed in the Tris-HCl buffer at pH 8.0. To a 5.00 mL volumetric flask, 1 mL of 10.0 mM Tris-HCl buffer, 250  $\mu\text{L}$  of  $1\text{ mg mL}^{-1}$  aqueous CDs and 250  $\mu\text{L}$  of 10.0 mM aqueous  $\text{FeCl}_3$  were sequentially added. After 5 min incubation at room temperature, an appropriate volume of stock ATP solution was added into the mixture to make the desired concentrations. The mixture was diluted with deionized water to the volume, mixed well and then incubated for 30 min at room temperature. Subsequently, the phosphorescence intensity of the solution was measured at  $\lambda_{\text{em}}/\lambda_{\text{ex}} = 440/360\text{ nm}$ .

### Determination of ATP in human blood plasma

Acetonitrile was first added to an equal volume of human blood plasma for protein precipitation. The mixture was centrifuged at 5000 rpm for 5 minutes and the supernatant was collected. ATP was spiked into the aliquots of supernatant and then the mixture was diluted to a particular volume to make 10-fold diluted human blood plasma that contains different concentrations of spiked ATP. Aliquots of ATP spiked 10-fold diluted human blood plasma (500  $\mu\text{L}$ ) were then processed with the aforementioned sensing procedure. Subsequently, the phosphorescence spectra were recorded.

## Results and discussion

### Morphological and structural characterizations of CDs

The CDs were prepared by use of a facile hydrothermal method.

The reaction was conducted by first condensing citric acid and ethylenediamine at  $200\text{ }^\circ\text{C}$  for 5 hours, whereupon they formed polymer-like CDs, which were then carbonized to form the CDs. The morphology and structure of CDs were confirmed by the analysis described in the following. The transmission electron microscopy (TEM) images (Fig. 1a and Fig. S1 in the ESI<sup>†</sup>) reveal the homogeneous CDs with spherical shape and almost uniform diameter, about 11.5 nm. Fig. 1b also reveals the apparent aggregation of CDs induced by  $\text{Fe}^{3+}$  ions, suggesting that CDs formed a chelate with  $\text{Fe}^{3+}$ , thereby quenching the phosphorescence. The Atomic Force Microscope (AFM) images (Fig. S2 in the ESI<sup>†</sup>) further indicates that the spherical CDs were well distributed. As seen from the FT-IR spectrum (Fig. S3 in the ESI<sup>†</sup>) that stretching vibrations of C-OH at  $3430\text{ cm}^{-1}$ , C-H at  $2923\text{ cm}^{-1}$ ,  $2850\text{ cm}^{-1}$ ,  $1476\text{ cm}^{-1}$  and a broad peak at  $1570\text{ cm}^{-1}$  originate from vibrations of aromatic C=C, asymmetric stretching vibrations of C-NH-C at  $1126\text{ cm}^{-1}$ , bending vibrations of N-H at  $1570\text{ cm}^{-1}$ , and the vibrational absorption band of C=O at  $1635\text{ cm}^{-1}$  suggest those CDs produced by citric acid and ethylenediamine containing C=C, C=O, -OH, -NH and -CH groups. Moreover,  $^1\text{H-NMR}$  spectroscopy was studied, in the  $^1\text{H NMR}$  spectrum (Fig. S4 in the ESI<sup>†</sup>), the signals in the range of 6.5–8.5 ppm, which correspond to aromatic ring hydrogen, were observed.

### Phosphorescence properties of CDs

The CDs were produced from condensing citric acid and ethylenediamine by use of a facile hydrothermal method under

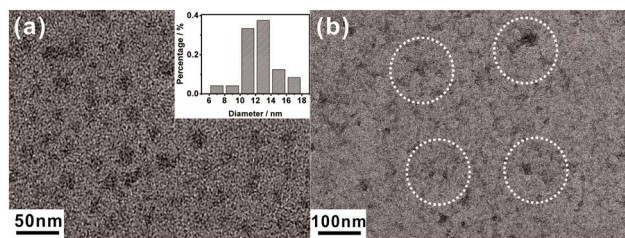


Fig. 1 TEM images of (a) CDs alone, the inset shows the size distribution of CDs and (b) CDs- $\text{Fe}^{3+}$ , apparent aggregation of CDs in white dotted circle.

different conditions in this work. As shown in Fig. 2 and 5d, the obtained CDs displayed a very strong photoluminescence including fluorescence with a short lifetime of 14.4 ns and high quantum yield to 75%, and phosphorescence with a long lifetime of 160  $\mu$ s. Excitation/solvent-dependent emission behaviour (Fig. S5 in the ESI<sup>†</sup>) was observed, which is common in fluorescent carbon-containing nanoparticles related with the surface state. In careful comparison to fluorescence characteristics, we found that the phosphorescence emission profile of CDs displayed only an enhancement in the longer wavelength region (500–600 nm) without the new emission band shifted to a long wavelength, similar to that of Mn doped ZnS quantum dots.<sup>6</sup> As demonstrated in the UV-Vis absorption spectrum (Fig. 2d), the peak centred at 240 nm is attributed to  $\pi$ - $\pi^*$  transition of C=C, and the peak at 350 nm is attributed to the  $n$ - $\pi^*$  transition of C=O. With the emission at 440 nm, the phosphorescence excitation spectrum shows a broad band from 300 to 400 nm and overlaps the band of C=O,<sup>23,24</sup> suggesting that the phosphorescence may come from the C=O bonds on carbon dots. In addition, as for the aromatic carbonyl group, the singlet and triplet states of the aromatic carbonyl group are close in energy, and the spin-orbit coupling is efficient, so that it is prone to intersystem crossing.<sup>5</sup> Therefore, it is reasonable to suppose that the phosphorescence originates from the aromatic carbonyl group on CDs. Moreover, it is well known that polycyclic aromatic hydrocarbons are a family of compounds which can be directly determined by room temperature phosphorimetry.<sup>8</sup> The phosphorescence of CDs is also possibly related to the graphitic structure which is similar to the polycyclic aromatic structure. Along with a serial of representative RTP emission spectra at different concentrations of CDs in water, no emission wavelength shift was observed even at the lowest concentration. A plot of the dependence of integrated RTP intensity versus nanoparticles concentration (or dilution factor) showing a good linear relationship is shown in the inset in Fig. 2c. This shows

that CDs were equally dispersed in water over a large concentration range. Substantial phosphorescence integrated intensities with good signal-to-noise ratios and well-resolved emission spectra were obtained with concentrations less than 1  $\mu$ g of particles per litre. Furthermore, a series of CD samples were collected under different reaction temperatures and ratios of precursors. Results showed that reaction temperature gave a significant effect on the phosphorescence intensity, while ratio of precursors had a slight effect (Fig. S6 in the ESI<sup>†</sup>). It is worthy to be noted that the photophysical characteristics described above are different from those of common organic small molecules. The corresponding clear-cut phosphorescence mechanism needs to be further studied in the future. The above results of the synthetic CDs with high stability and high luminescence quantum yield in aqueous solution were in favour of phosphorescence sensing and detection.

### Effects of pH on the sensing of ATP

The effects of pH on the phosphorescence intensity of the CD sensing system were investigated (Fig. 3). Phosphorescence intensities of CDs only remain nearly constant over a wide range of pH from 4.0 to 9.5 without changes in RTP emission profile. The mixture solution of CDs and iron ions was observed with the naked-eye. Precipitation occurred at a pH higher than 8.0 due to hydrolysis, accompanied with the weakness of the quenching capacity of  $\text{Fe}^{3+}$ . However, for ATP sensing, a larger phosphorescence recovery could be obtained at higher pH. In view of a comprehensive consideration of sensitivity and reproducibility, a 10 mM Tris-HCl buffer of pH 8.0 was recommended to be used throughout.

### Selectivity of the CD-based phosphorescence method

The considerable phosphorescence of the CDs was found to be selectively quenched in the presence of  $\text{Fe}^{3+}$ .<sup>22</sup> In addition, the effects of various of other metal ions were investigated including  $\text{K}^+$ ,  $\text{Na}^+$ ,  $\text{Li}^+$ ,  $\text{Ca}^{2+}$ ,  $\text{Mg}^{2+}$ ,  $\text{Mn}^{2+}$ ,  $\text{Ba}^{2+}$ ,  $\text{Cu}^{2+}$ ,  $\text{Pb}^{2+}$ ,  $\text{Ag}^+$ ,  $\text{Zn}^{2+}$ ,  $\text{Cd}^{2+}$ ,  $\text{Co}^{2+}$ ,  $\text{Ni}^{2+}$  and  $\text{Fe}^{2+}$ . As shown in Fig. 4a, only  $\text{Fe}^{3+}$  brought about the marked phosphorescence quenching. The phosphorescence of CDs gradually decreased when the concentration of  $\text{Fe}^{3+}$  ions increased. The quenching effect presumably results from the effective electron transfer that occurs from carboxyl and hydroxyl group functionalized CD

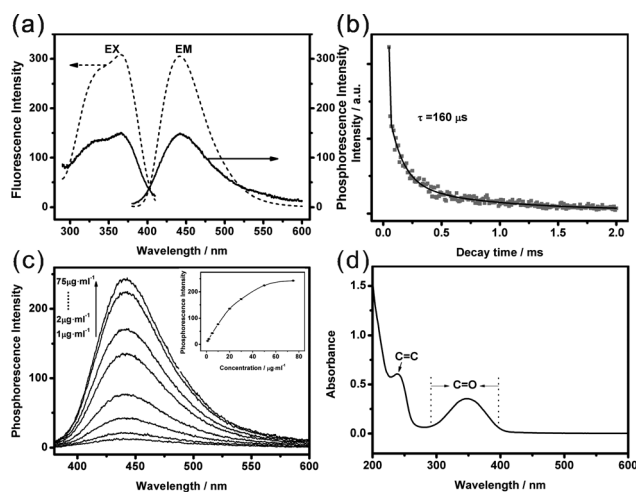


Fig. 2 (a) Phosphorescence spectra (solid line) and fluorescence spectra (dash line) of CDs. (b) Time resolved phosphorescence decay by delay of CDs. (c) RTP emission profiles of different concentrations of CDs. (d) The UV-Vis absorption spectrum of CDs dispersed in water.

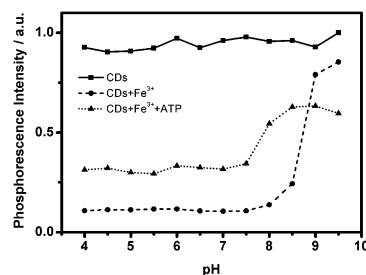


Fig. 3 Effect of pH on the phosphorescence intensity of CDs ( $50 \mu\text{g mL}^{-1}$ ) only, CDs ( $50 \mu\text{g mL}^{-1}$ ) +  $\text{Fe}^{3+}$  ( $500 \mu\text{M}$ ) and CDs ( $50 \mu\text{g mL}^{-1}$ ) +  $\text{Fe}^{3+}$  ( $500 \mu\text{M}$ ) + ATP ( $1200 \mu\text{M}$ ), respectively.

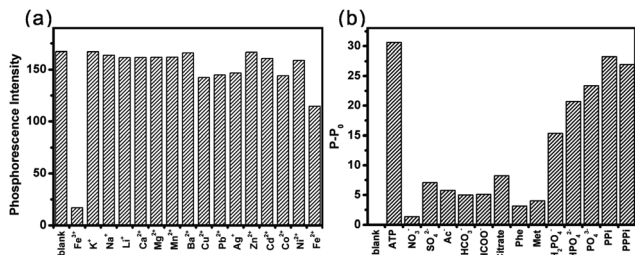


Fig. 4 (a) Phosphorescence intensity of CDs ( $50 \mu\text{g mL}^{-1}$ ) after addition of different metal ions ( $500 \mu\text{M}$ ). (b) Phosphorescence enhancement of CDs ( $50 \mu\text{g mL}^{-1}$ )- $\text{Fe}^{3+}$  ( $500 \mu\text{M}$ ) system up addition of different anions ( $100 \mu\text{M}$ ).  $P$  and  $P_0$  are phosphorescence intensity with and without anions, respectively.

complexation with  $\text{Fe}^{3+}$ . The quenching effect presumably results from that the CDs and  $\text{Fe}^{3+}$  formed non-luminescent chelate. Besides, it is widely known that phosphate ions give a considerable affinity to iron ions through  $\text{Fe-O-P}$  bonds.<sup>21,25</sup>

Therefore, the quenching phosphorescence of CDs caused by  $\text{Fe}^{3+}$  can be recovered in the presence of phosphate-containing molecules. Hence, we further evaluated the selectivity of the “off-on” phosphorescence approach to familiar anions such as  $\text{NO}_3^-$ ,  $\text{SO}_4^{2-}$ ,  $\text{Ac}^-$ ,  $\text{HCO}_3^-$ , formate, citrate, phenylalanine, methionine,  $\text{H}_2\text{PO}_4^-$ ,  $\text{HPO}_4^{2-}$ ,  $\text{PO}_4^{3-}$ , pyrophosphate and triphosphate. As indicated in Fig. 4b, ATP has the greatest effect on the restoration of the phosphorescence that is quenched by  $\text{Fe}^{3+}$ .

Moreover, it is notable that multiposphates show higher affinity to  $\text{Fe}^{3+}$  than monophosphates (Fig. S8 in the ESI†).

### Incubation time and time-resolved phosphorescence decay assays

To evaluate the effect of incubation time, the phosphorescence intensity as a function of time was monitored. As illustrated in Fig. S9 (in the ESI†), the chelation between CDs and  $\text{Fe}^{3+}$  was a quite rapid process that reached equilibrium in 5 min. While the formation and release of the  $\text{ATP-Fe}^{3+}$  complex from CDs was relatively slow and achieved equilibrium in almost 30 min. As seen from Fig. S7 (in the ESI†) that the linear relationship between  $(P_0 - P)$  and concentration of  $\text{Fe}^{3+}$  ions shows that the phosphorescence quenching follows the Lineweaver-Burk equation well, while the relationship between  $P_0/P$  and the concentration of  $\text{Fe}^{3+}$  does not follow Stern-Volmer's Equation. According to references, the dynamic quenching can be described by Stern-Volmer's equation, while the static quenching conforms to the Lineweaver-Burk equation.<sup>6</sup> Thus, it is reasonable to suppose that RTP of CDs quenched by  $\text{Fe}^{3+}$  ions was in agreement with a static quenching model. To better understand the RTP “off-to-on” mechanism for sensing ATP, time-resolved phosphorescence and fluorescence decay of CDs in the presence of  $\text{Fe}^{3+}$  and ATP were studied, respectively. Decay profiles are shown in Fig. 5. The phosphorescence lifetime of free CDs is about  $160 \mu\text{s}$ , while a slight increment of lifetime of  $166 \mu\text{s}$  was observed in the presence of  $\text{Fe}^{3+}$  ions, and the subsequent addition of ATP, with a lifetime of  $159 \mu\text{s}$ . A

similar trend has also been observed in the time-resolved fluorescence decay profile. Besides, phosphorescence lifetime of different concentration of CDs was shown in Fig. S10 (in the ESI†), suggesting that the concentration of CDs has little impact on the phosphorescence lifetime. These results described above suggest that the phosphorescence quenching mechanism of CDs by  $\text{Fe}^{3+}$  was attributed to a static quenching process resulting from the formation of non-luminescent chelate, and then the dissociation of  $\text{Fe}^{3+}$  from CDs by the phosphate species through strong interactions.

### Sensitivity of the sensing system

To demonstrate that the present system can be applied in sensing of ATP, the phosphorescence responses to ATP at different concentrations were measured under optimum conditions. The phosphorescence emission spectra of the system upon the addition of different concentrations of ATP ranging from 20 to  $1200 \mu\text{M}$  were shown in Fig. 6a. Fig. 6b shows a dramatic increment of the phosphorescence intensity as the concentration of ATP increased. Meanwhile, inset of Fig. 6b clearly illustrates the corresponding calibration curve plot between the phosphorescence intensity enhancement factors  $(P - P_0)$  against the ATP concentration. The linear working concentration range was found to be  $20\text{--}200 \mu\text{M}$ . The regression equation is  $Y = 0.113X + 1.398$ , with correlation coefficient ( $R^2$ ) of 0.994. Moreover, the limit of detection (LOD) was estimated to be  $14 \mu\text{M}$  ( $3\sigma/S$ ), in which  $\sigma$  is the standard deviation for the blank solution ( $n = 6$ ), and  $S$  is the slope of the calibration curve.

### Measuring ATP in real blood plasma samples

In order to evaluate the applicability of the proposed CDs based RTP “off-to-on” sensing approach, ATP assay in real human blood plasma sample was further studied. As shown in Fig. 7a, the fluorescent background of blood plasma was significant

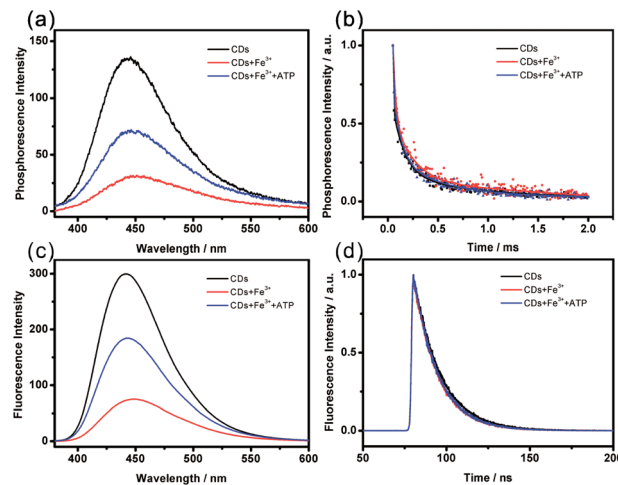


Fig. 5 (a) State phosphorescence spectra and time-resolved phosphorescence decay (b) of CDs alone, CDs +  $\text{Fe}^{3+}$ , and CDs +  $\text{Fe}^{3+}$  + ATP; (c) state fluorescence spectra and time-resolved fluorescence decay (d) of CDs alone, CDs +  $\text{Fe}^{3+}$ , and CDs +  $\text{Fe}^{3+}$  + ATP.

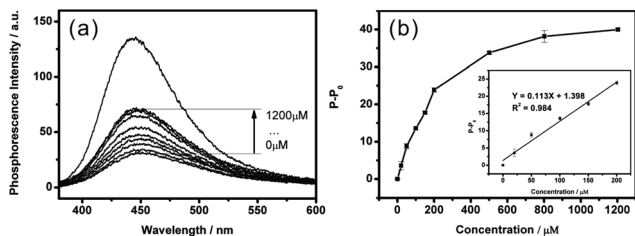


Fig. 6 (a) Phosphorescence emission spectra of CDs-Fe<sup>3+</sup> (50 μg mL<sup>-1</sup>–500 μM) in the presence of different concentrations of ATP (0, 20, 50, 100, 150, 200, 500, 800, 1200 μM). (b) The relationship between  $(P - P_0)$  and the concentration of ATP.  $P$  and  $P_0$  are phosphorescence intensity with and without ATP, respectively.

(black line), while no background was observed in the phosphorescence mode (red line). Since only very few species are able to emit analytically useful phosphorescence at room temperature,<sup>8</sup> the long delay time of phosphorescence can simply avoid the interference from the scattering light and undesired fluorescence emission.

A standard addition method was applied to estimate the ATP concentration in human blood plasma. Different concentrations of ATP were spiked into the 10-fold diluted human blood plasma and were further incubated with the CDs-Fe<sup>3+</sup> sensing system under the optimal conditions. In the test solution, human blood plasma was finally diluted 100-fold and the spiked ATP was at a concentration of 0, 20, 50, 100, 150 μM. The blood plasma samples from 2 healthy volunteers were measured and the results are shown in Fig. 7b. It was found that the present approach provides a linear response to ATP spiked into human blood plasma, and the regression equations are  $Y = 0.102X + 6.903$  and  $Y = 0.083X + 3.422$ , with correlation

coefficients ( $R^2$ ) of 0.991 and 0.993 respectively (Fig. 7c and d). Using the standard addition method, we estimated that the concentrations of ATP of the 2 human blood plasma samples are 6.77 mM and 4.07 mM respectively. As previously mentioned, the physiological concentration of blood phosphates is at a millimolar level, and is mainly dominated by ATP. Thus we considered that ATP was mainly responsible for the phosphorescence recovery in the sensing process. Consequently, the proposed sensing system can be used to evaluate the health conditions of individuals.

## Conclusions

In summary, we have demonstrated a novel RTP method based on the phosphorescence property of CDs for the cost-effective, readily, sensitive detection of ATP, the main phosphate-containing metabolite in human blood plasma. The phosphorescence emission centred at 440 nm with an average lifetime of 160 μs under excitation of 360 nm can be quenched in the presence of Fe<sup>3+</sup> attributing to nonradiative electron transfer and then turned on by the phosphate ions through the strong interactions. Deoxidants and other inducers that are necessary in conventional RTP detection and interferences from autofluorescence and the scattering light of the complex matrix encountered in spectrofluorometry could be readily avoided in the presence of CD-based RTP. Combinations of varieties of interactions between metal ions and surface ligands of CDs and the desirable phosphorescence properties show that water-soluble and biocompatible CDs are promising for RTP chemical and biological sensing and time-resolved imaging. Moreover, CD-based RTP nanocomposites could potentially be used in anti-counterfeiting, especially for food and drugs.

## Acknowledgements

The authors gratefully acknowledge the financial support for this work from the National Natural Science Foundation of China (Grant no. 21305161), the Natural Science Foundation of Jiangsu Province (Grant no. BK20130643).

## Notes and references

- 1 C. Q. Ding, A. W. Zhu and Y. Tian, *Acc. Chem. Res.*, 2013, **47**, 20–30.
- 2 Y. P. Sun, B. Zhou, Y. Lin, W. Wang, K. A. Fernando, P. Pathak, M. J. Meziari, B. A. Harruff, X. Wang, H. Wang, P. G. Luo, H. Yang, M. E. Kose, B. Chen, L. M. Veca and S. Y. Xie, *J. Am. Chem. Soc.*, 2006, **128**, 7756–7757.
- 3 H. Ding, L. W. Cheng, Y. Y. Ma, J. L. Kong and H. M. Xiong, *New J. Chem.*, 2013, **37**, 2515–2520.
- 4 K. G. Qu, J. S. Wang, J. S. Ren and X. G. Qu, *Chemistry*, 2013, **19**, 7243–7249.
- 5 Y. Deng, D. Zhao, X. Chen, F. Wang, H. Song and D. Shen, *Chem. Commun.*, 2013, **49**, 5751–5753.
- 6 Y. He, H. F. Wang and X. P. Yan, *Anal. Chem.*, 2008, **80**, 3832–3837.

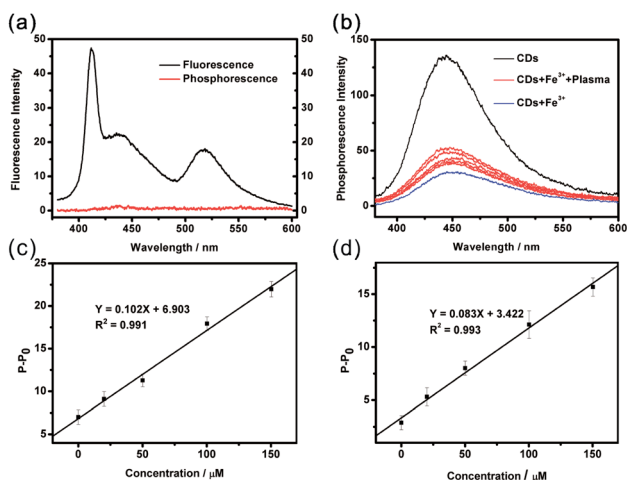


Fig. 7 (a) RTP (red line) and fluorescence (black line) spectra of human blood plasma. (b) Representative phosphorescence emission spectra of CDs (50 μg mL<sup>-1</sup>)-Fe<sup>3+</sup> (500 μM) in the presence of 100-fold diluted human blood plasma spiked with different concentrations of ATP (0, 20, 50, 100 and 150 μM). (c and d) The corresponding relationship between  $(P - P_0)$  and the concentration of spiked ATP in the two human blood plasma samples.

- 7 Q. Zhao, C. Huang and F. Li, *Chem. Soc. Rev.*, 2011, **40**, 2508–2524.
- 8 A. S. Castillo, A. S. Carretero, J. C. Fernández, W. J. Jin and A. F. Gutiérrez, *Anal. Chim. Acta*, 2004, **516**, 213–220.
- 9 E. Sotelo-Gonzalez, L. Rocas, S. Garcia-Granda, M. T. Fernandez-Arguelles, J. M. Costa-Fernandez and A. Sanz-Medel, *Nanoscale*, 2013, **5**, 9156–9161.
- 10 X. J. Mao, H. Z. Zheng, Y. J. Long, J. Du, J. Y. Hao, L. L. Wang and D. B. Zhou, *Spectrochim. Acta, Part A*, 2010, **75**, 553–557.
- 11 X. Michalet, F. F. Pinaud, L. A. Bentolila, J. M. Tsay, S. Doose, J. J. Li, G. Sundaresan, A. M. Wu, S. S. Gambhir and S. Weiss, *Science*, 2005, **307**, 538–544.
- 12 L. P. Lin, X. X. Wang, S. Q. Lin, L. H. Zhang, C. Q. Lin, Z. M. Li and J. M. Liu, *Spectrochim. Acta, Part A*, 2012, **95**, 555–561.
- 13 G. V. Zyryanov, M. A. Palacios and P. Anzenbacher, *Angew. Chem., Int. Ed.*, 2007, **46**, 7849–7852.
- 14 J. R. Knowles, *Annu. Rev. Biochem.*, 1980, **49**, 877–919.
- 15 F. Liu, J. Zhang, R. Chen, L. Chen and L. Deng, *Chem. Biodiversity*, 2011, **8**, 311–316.
- 16 N. Azorin, M. Raoux, L. Rodat-Despoix, T. Merrot, P. Delmas and M. Crest, *Exp. Dermatol.*, 2011, **20**, 401–407.
- 17 P. H. Li, J. Y. Lin, C. T. Chen, W. R. Ciou, P. H. Chan, L. Luo, H. Y. Hsu, E. W. G. Diao and Y. C. Chen, *Anal. Chem.*, 2012, **84**, 5484–5488.
- 18 W. Tedsana, T. Tuntulani and W. Ngeontae, *Anal. Chim. Acta*, 2013, **783**, 65–73.
- 19 H. N. Lee, Z. Xu, S. K. Kim, K. M. K. Swamy, Y. Kim, S. J. Kim and J. Yoon, *J. Am. Chem. Soc.*, 2007, **129**, 3828–3829.
- 20 L. N. Zhong, F. F. Xing, Y. L. Bai, Y. M. Zhao and S. R. Zhu, *Spectrochim. Acta, Part A*, 2013, **115**, 370–375.
- 21 J. J. Liu, X. L. Zhang, Z. X. Cong, Z. T. Chen, H. H. Yang and G. N. Chen, *Nanoscale*, 2013, **5**, 1810–1815.
- 22 S. J. Zhu, Q. N. Meng, L. Wang, J. H. Zhang, Y. B. Song, H. Jin, K. Zhang, H. C. Sun, H. Y. Wang and B. Yang, *Angew. Chem.*, 2013, **52**, 3953–3957.
- 23 O. Bolton, K. Lee, H. J. Kim, K. Y. Lin and J. Kim, *Nat. Chem.*, 2011, **3**, 205–210.
- 24 B. J. Clark, T. Frost and M. A. Russell, *UV Spectroscopy: Techniques, Instrumentation, Data Handling/UV Spectrometry Group*, Chapman & Hall, London, New York, 1993, vol. 4.
- 25 J. A. Simmons, *Water, Air, Soil Pollut.*, 2010, **209**, 123–132.